CPG and Tegotae-based Locomotion Control of Quadrupedal Modular Robots

Rui Vasconcelos
rui.vasconcelos@tecnico.ulisboa.pt

Instituto Superior Técnico, Lisboa, Portugal

November 2016

Abstract

Animals exhibit astonishing capabilities in terms of locomotion control which Science aims at understanding and reproducing in robots. The ability to adapt movements based on morphological changes is specially interesting in the field of reconfigurable robotics. It is commonly accepted that two components play an important role in the way animals perform control: Central Pattern Generators and Reflex Mechanisms. Respectively, two bio-inspired control strategies were studied under the scope of this work, an optimized open loop CPG network, and a closed loop decentralized control of the limbs by Tegotae feedback rules. A quadruped robotic platform was chosen for the study, being modelled in *Webots* simulator, where optimization and search algorithms were employed, and implemented on hardware, where validation experiments took place. The focus of this project was on analyzing performance of imposed gaits, with the first strategy, comparing it with emergent gaits from the decentralized approach. This comparison proved that Tegotae-based control is able not just to drive the system towards a stable steady state limit cycle behaviour, as it does so for a near optimal one. Several gaits found in nature were reproduced with a simple trajectory parametrization method, indicating energetic cost and mechanical stability of these. Tegotae-based control was thoroughly analyzed, and some improvements are proposed, namely scaling with frequency and variable attraction coefficient. Binary feedback was also put at proof for the first time, showing feasibility but some performance loss. Diverse software and hardware tools were developed for use in future work.

Keywords: CPG, Tegotae, Decentralized Control, Emergent Gaits, Quadruped.

1. Introduction

In the last few years, with the growth of fields of research such as Biorobotics, diverse bio-inspired control approaches have been developed with the goal of understanding animal locomotion behaviour and replicate it in robots. From the control point of view, one of the most interesting features developed in nature through evolution is the competence for adaptability of movements to: morphological changes experienced during the animal lifecycle, surrounding environment, and desired speed of locomotion (e.g. gait transitions to avoid frequency saturation by the limbs). Specially in the field of modular reconfigurable robotics, the desire for control methods capable of adaptation to morphological changes is high, and bio-inspired techniques may present valid advantages against classical control strategies.

In the scope of this thesis work, two of these bio-inspired techniques were studied, having as subject a quadrupedal modular robot, an optimized open loop approach based on Central Pattern Generators (CPG) and a decentralized closed loop strategy based on sensory feedback denominated Tegotae.

2. Background

The underlying control methods used by animals seem to follow universal principles, being commonly accepted that four main ingredients play an important role:

1. A simple descending modulation from the brain, responsible for the locomotion trigger, which has been reproduced by electrical stimulation of a section of the brain stem denominated Mesencephalic Locomotor Region (MLR).

2. Central Pattern Generators (CPG), neural circuits found in both vertebrates and invertebrates that transform simple non-periodic descending stimulus from the brain into periodic locomotion movements, rhythmic patterns.

3. Reflex mechanisms based on sensory feedback, responsible for the adaptation of movements.

4. Robust body mechanics necessary for stability, which include compliance and consequent passive dynamics, helpful for the execution of dynamical gaits.

With an inspiration on the described components of animal locomotor control, several strategies have been developed based on the concept of CPG and reflex mechanisms. Modelled by networks of phase-oscillators, CPG-based techniques have been employed to diverse control applications, from salamander [1], to quadruped [2] [3] [4], to humanoid robots [5] [6] [7] to exoskeletons [8] – see [9] for an overview. In a similar fashion, a first strategy used in this thesis relies on such concept, with an open loop control, optimized recurring to Particle Swarm Optimization.

A second control approach employed in this master project is based on local reflex mechanisms, using external feedback to affect the limb phase through a Tegotae rule, in a decentralized fashion. Tegotae based control has been shown to result on the visualization of emergent gaits (diagonal sequence walk, lateral sequence walk, trot, pace, rotary gallop and bound) and gait transitions [10] by a decentralized control of each limb, with adaptation to the dynamical characteristics of the robot such as weight distribution [11] [12].

With open loop CPG it is possible to control any morphology given a prior optimization process, however computationally expensive re-optimizations are needed after reconfiguration. With decentralized Tegotae feedback rules, emerging gaits are visualized, not being however clear what are the boundaries within which there is convergence to limit cycle behaviour, nor the quality of the solution, when compared with the optimized one. Hence, the focus of this project was to compare performance of these strategies in terms of speed, energy efficiency and mechanical stability, analyzing effect of step trajectories and showing feasibility of convergence to stable limit cycle behaviour.

3. Methods

In order to study the performance of these control strategies, a choice for a simple morphology was taken, resulting in a robotic platform composed by symmetric planar limbs with two degrees of freedom, whose model was developed in *Webots* dynamics simulator and hardware implemented as shown in figure 1.

These control strategies were implemented considering a step trajectory predefined in cartesian space to be followed through inverse kinematics, being proposed a simple parametrization method

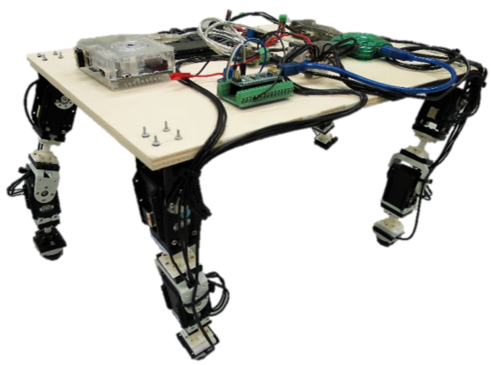

Figure 1: Robotic platform implemented on hardware – sensory information includes ground reaction force, inertial measurements (IMU) and current drawn by the motors.

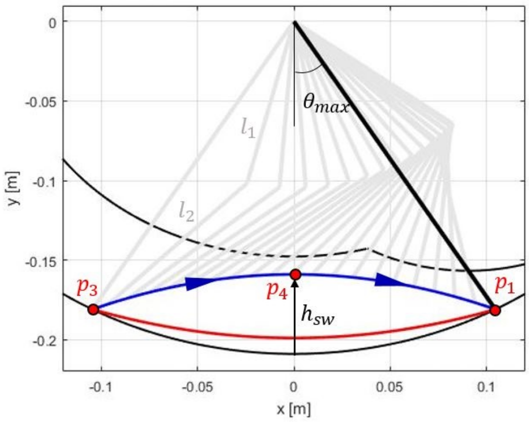

Figure 2: Parametrized step trajectory: swing phase – θ_{max}, h_{sw}. Limb workspace drawn in black.

based on the workspace of each limb and defined by quadratic curves of stance and swing phases. Figure 2 describes this parametrization method for swing phase and stance is obtained in the same fashion considering a parameter for height of stance h_{st} that defines a mid-point p_2.

3.1. Open Loop CPG-based control

The open loop approach is based on a network of coupled phase-oscillators (figure 3(a)), with one oscillator per limb where the phase of each limb is directly correlated to the position in cartesian space of the trajectory (figure 4(a)). This correspondence is reshaped by a transition phase ϕ_t, in order to impose a duty factor. The phase of each limb, ϕ_i is then given by a set of coupled differential equations described as:

$$\dot{\phi}_i = 2\pi f + \sum_j w_{ij} \sin(\phi_j - \phi_i - \psi_{ij}) \qquad (1)$$

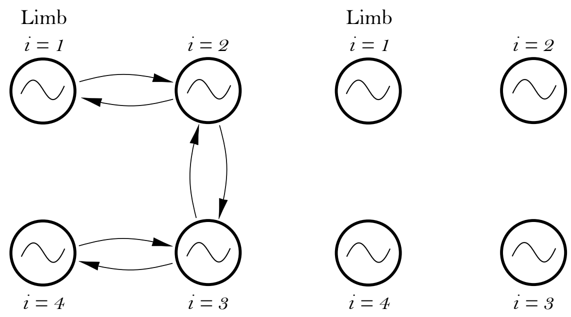

(a) Open Loop CPG. (b) Tegotae.

Figure 3: Networks of phase-oscillators – one oscillator per limb coupled in the case of open loop CPG and no coupling in the case of Tegotae.

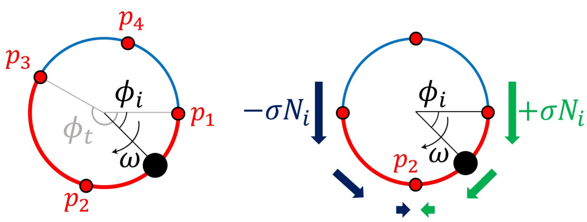

(a) Open Loop CPG. (b) Tegotae.

Figure 4: Transformation from limb phase ϕ_i to trajectory in cartesian space – effect of force feedback shown in the case of Tegotae for steady state.

Where the desired phase shift between limbs i and j, ψ_{ij} is optimized along side with the trajectory parameters θ_{max}, h_{st} and h_{sw}, and the imposed duty factor, described as df.

During a transient phase, the coupling between oscillators will have an important effect on driving the system from an arbitrary initial condition to a steady state one, where phase-locking occurs and all limbs oscillate at the same frequency $\omega = 2\pi f$.

3.2. Tegotae-based Control

In the case of Tegotae, this is implemented as separate phase-oscillators (figure 3(b)), controlled in a decentralized fashion, by an attraction to a stable point p_2, proportional to the normal ground reaction force N_i, with a slope given by attraction coefficient σ (figure 4(b)). The phase rate of each limb is in this case given by the differential equation 2.

$$\dot{\phi}_i = 2\pi f + \sigma \, N_i \, \cos(\phi_i) \qquad (2)$$

During transient, some force feedback from the ground may occur during swing phase, however, the attraction created by the second term of equation 2 will push the phase in the direction of stance. These corrections of phase, aided by the dynamics of the body, will create a physical communication between limbs, and drive the system towards a steady state gait, where force feedback is experienced only during stance phase, as exhibited in figure 4(b).

In this work it was also studied the possibility of using only binary feedback, of touching or not the ground, being implemented as in equation 3, where a threshold of 0.2N was considered to avoid incorrect classifications due to noise.

$$\dot{\phi}_i = 2\pi f + \sigma_b \, B_i \, \cos(\phi_i) \qquad (3)$$

$$B_i = \begin{cases} 1 & \text{if } N_i > 0.2 \text{ N} \\ 0 & \text{if } N_i < 0.2 \text{ N} \end{cases} \qquad (3)$$

3.3. Fitness Computation

With a view to allow the usage of optimization and search algorithms, and suppress the need to analyze the time response correspondent to each set of parameters, a group of system response metrics were defined, being here exposed the most relevant.

Discrete time is considered with time step T, in a way that simulation starts at $kT = 0$, measurements start at $t = t_m = k_m T$ to consider only steady state , and finally runtime finishes at $k = k_e$.

One important metric considered was the distance traveled during measurement time, and correspondent average speed, respectively given by:

$$D_t = \|\overrightarrow{x_{CM}}(k_e T) - \overrightarrow{x_{CM}}(k_m T)\| \qquad (4)$$

$$\overline{v_{CM}} = \frac{D_t}{k_e T - k_m T} \qquad (5)$$

In addition, energetic cost metrics were used, in a different manner in simulation and hardware. In the first case, mechanical power was considered as expressed in equation 6, where a robot with n limbs of m degrees of freedom was considered. $\dot{\vartheta}_{j,i}$ and $\tau_{j,i}$ designate respectively joint speed and torque of degree of freedom j, part of limb i. Total energy consumption during measured experiment time is obtained by equation 7.

$$P_m(kT) = \sum_{i=1}^{n} \sum_{j=0}^{m} |\dot{\vartheta}_{j,i}(kT) \cdot \tau_{j,i}(kT)| \qquad (6)$$

$$E_t = \sum_{k=k_m}^{k_e} P_m(kT) \qquad (7)$$

On the other hand, for hardware, the energetic cost considered was directly the one used for the motors actuation. As the experimental setup included a power source with constant input voltage

$V_{in} = 18$V, the input current I_{in} was measured for every time step, and the total cost is given by:

$$E_t = \sum_{k=k_m}^{k_e} V_{in} \cdot I_{in}(kT) \tag{8}$$

Finally, the gait energy efficiency, ϵ_t, is defined as the inverse of the cost of transport (CoT), indicating how much distance can be traveled using the specified gait with one unity of energy.

$$\epsilon_t = CoT^{-1} = D_t/E_t \tag{9}$$

Additional performance indicators were considered, describing mechanical stability, convergence levels and number os step cycles, not being however used as fitness for optimization and search methods.

4. Experiments

With the goal of increasing the understanding on how step trajectories, duty factor, and phase shift between limbs should be fixed to result in stable and efficient locomotion methods, two problems were solved repetitively using Particle Swarm Optimization (PSO), in a total of 41 optimizations. The search problems are below described, with omission of the boundary conditions of each parameter, having trajectory parameters bounded by the workspace, $df \in [0, 1]$ and $\psi_{ij} \in [-\pi, \pi]$.

1. Energy efficiency PSO for constant frequency $f_d \in (0.5, 1, 1.5)$ Hz:

   Maximize:

   $$Z(\theta_{max}, h_{st}, h_{sw}, df, \psi_{12}, \psi_{23}, \psi_{34}) = \epsilon_t$$

   Subject to:

   $$f = f_d \qquad (...)$$

2. Two-stage PSO: energy minimization for desired speed $v_d \in (0.25, 0.5, 0.75, 1)\; m \cdot s^{-1}$:

   Maximize:

   $$Z(f, \theta_{max}, h_{st}, h_{sw}, df, \psi_{12}, \psi_{23}, \psi_{34}) = \frac{1}{E_t}$$

   Subject to:

   $$\overline{v_{CM}} \geq v_d \qquad (...)$$

Posteriorly, and given the results of the optimization process (see 5.1), the search for near-optimal locomotion was restricted to trot gait, leading to:

3. Systematic Search of Trot Gaits – θ_{max}, h_{sw}, f, df.

Regarding Tegotae-based control, the search parameters were restricted to four, and a systematic search was performed in the same fashion:

4. Systematic Search on Tegotae-based Control – θ_{max}, h_{sw}, f, σ.

These conclude the procedures executed in simulation, which lead to validation tests on hardware. Additional experiments on hardware were performed, being the most relevant:

5. Search on Trajectory: effect of θ_{max} and h_{sw} on imposed trot gaits;

6. Analysis of effect of σ in convergence time;

7. Search on σ *versus* frequency;

8. Convergence and steady state analysis of binary feedback.

5. Results

5.1. Optimization of Open Loop CPG network

Considering experiment 1, the solutions showed that very slow trot gaits are the most energy efficient, with stretched knee in all the step cycle ($h_{st} \approx 0$, $h_{sw} \approx 0$), creating ground clearance through body dynamics and including very high duty factors. However, both in nature and robotics, it is desired to travel at a speed which is not too reduced.

With a view on confirming the validity of the obtained solutions, convergence of particles during the optimization procedure is verified. An example is shown in figure 5.

Adding then a lower boundary for the locomotion speed v_d, the resulting gaits of the second type of optimization procedure are expressed in figure 6. Focusing on such results, it is visible that the increase of minimum cost is proportional to the one of desired speed.

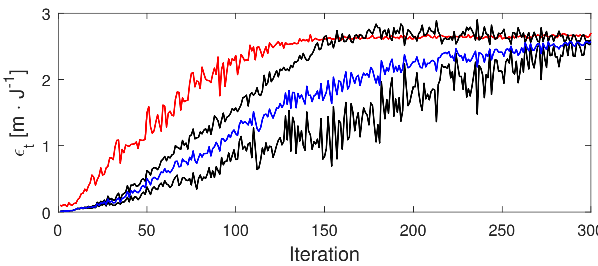

Figure 5: Convergence of solutions during PSO to maximize energy efficiency – fitnesses of top particle in red, average of all 50 particles in blue and in black average ± variance.

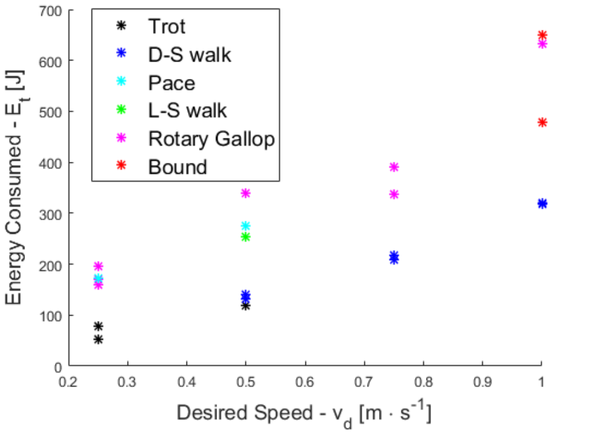

Figure 6: Energy consumption of gaits derived from two-stage Particle Swarm Optimization versus desired speed v_d – 6 gaits encountered.

At lower speeds, up to 0.5 meters per second, trot gaits are present, being then replaced by diagonal sequence walk (D-S walk) as the least expensive locomotion method. Even without limb saturation, the natural frequencies of the body dynamics do not allow trot gaits faster than a certain speed, converging in this case to a less stable limit cycle of D-S walk. The pendular of walking trot (roll *versus* pitch) is expressed in figure 7(a), where the presence of a very stable limit cycle is shown.

With higher energetic cost, a second group of gaits appear, where the body dynamics has an increased influence. Such group is characterized by using the knee in an inverted way as before, showing bending at stance, and stretching during swing. A push-off is created, which inputs energy to the system dynamics. In an initial phase, where speeds are $v_d \in [0.25, 0.5]$, these gaits are less stable, showing a stepping order that corresponds to pace and L-S walk. However, as the desired speed increases, running gaits with a much more stable limit cycle behaviour tend to appear, such as rotary gallop or bound, whose pendular behaviour is expressed in figures 7(b) and 7(c).

The variety of solutions, aided by proof of convergence, indicates the clear presence of a non-convex problem with several local optima.

Despite the diverse gaits obtained, trot is the most energy efficient one, besides constrained to certain speed limits, and transitions to highly dynamical running gaits are complex and out of the scope of this project. In addition, the relative quality of trot gait was analyzed on hardware, for a fixed frequency and trajectory, with results shown in table 1, being clear the advantage of trot against other symmetrical walking gaits found in nature. A local analysis on trot was also performed showing that it represents as well a local optima.

Table 1: **Hardware:** comparative analysis of symmetrical walking gaits showing advantage of trot.

Imposed Gait	$\overline{v_{CM}}$ $[m \cdot s^{-1}]$	ϵ_t $[m \cdot kJ^{-1}]$
Trot	0.059	4.042
D-S walk	0.035	1.583
L-S walk	0.032	1.87

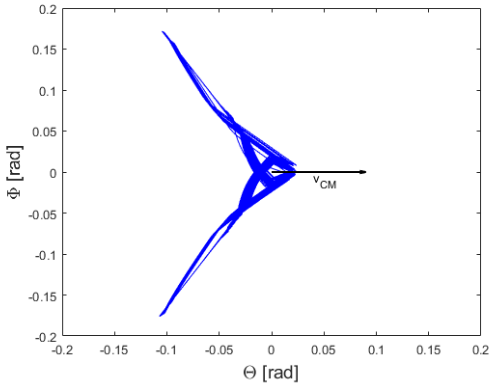

(a) Walking trot.

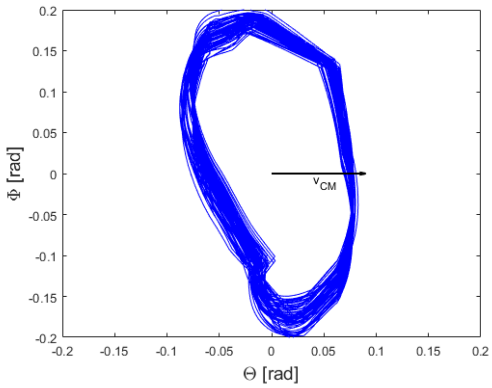

(b) Rotary gallop.

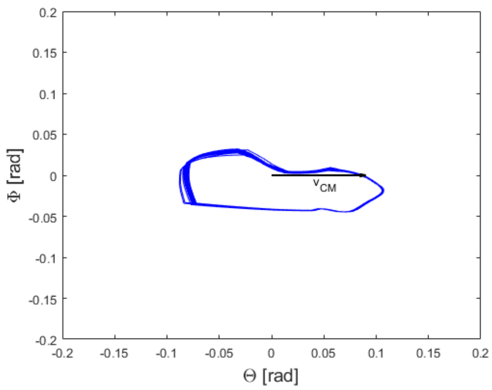

(c) Bound.

Figure 7: **Simulation:** Limit cycle behaviour of dynamical gaits, analyzed on roll (Φ) and pitch (Θ), representing the path followed by an inverted pendulum fixed to the upper body of the robot.

With such motivation, and taking into consideration that the decentralized control approach (Tegotae), drives our robotic system towards trot gaits, this was the type of locomotion considered for the following study on trajectories and duty factor. In such study, h_{st} was considered null and $df \in [0.5, 1]$, as they beneficial in terms of energy efficiency. This conclusion was result of the optimization process and later validated on hardware.

5.2. Systematic Search of imposed Trot gaits – θ_{max}, h_{sw}, f, df

Considering the 4 different parameters under study, as well as the fitness values of average speed, energy efficiency and mechanical stability, 7-dimensional data had to be analyzed to understand correlations and trends. Splitting the data in different frequencies, and using color as a forth dimension, visualization of the results is possible, as done in figure 8 for speed and energy efficiency of gaits with frequency $f = 0.25$ Hz.

As shown in the results of PSO, it is here visible that small steps are the ones that show more energy efficiency, but no speed. Hip amplitude θ_{max} seems to correlate almost linearly with speed, independently of h_{sw}, which is only necessary to create ground clearance for $\theta_{max} > 0.4$ and for $df \approx 0.5$. However, h_{sw} does affect energy efficiency, showing that a minimum value to create ground clearance for a fixed θ_{max}, but not bigger, should be used.

Regarding the effect of imposed duty factor df, a value around 0.5 seems to benefit speed, having a negative consequence proportional to the increase of this parameter. Such result can be explained by higher velocities during transition from swing to stance, which create collisions and opposite forces to the direction of movement. In terms of energy efficiency, values ranging from 0.55 to 0.8 are preferable, depending on the trajectory parameters.

A validation of such results was performed on hardware considering only $f = 0.25$ Hz and $df = 0.5$. In terms of average traveling speed, an almost perfect fit of the curve shown in figure 8(a) was visualized. However, regarding energy the different methods of computation of energetic cost imply that they are not comparable. In simulation the mechanical power is used to compute energetic cost by equation 7, however, on hardware, the current is measured at a time step of $1ms$ and integrated in time, using equation 8 for total energy computation. The difference relies on the fact that, on the robotic platform, a base current is drawn from the motors even if the robot is stopped, which corresponds to zero energy consumption in simulation.

How to proceed in such a case is fully dependent on the goal. If the goal is to understand animal locomotion, this base current should not be accounted

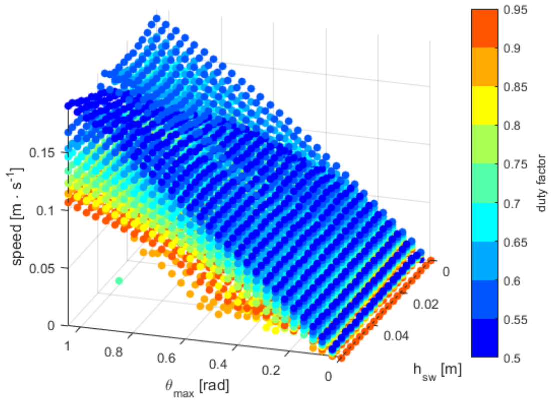

(a) Average speed as a function of θ_{max}, h_{sw} and df.

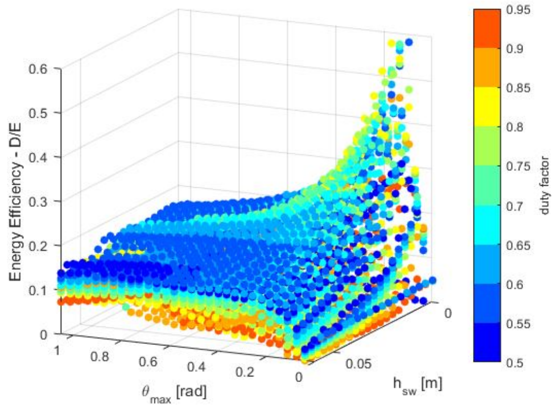

(b) Energy efficiency $(m \cdot J^{-1})$ as a function of θ_{max}, h_{sw} and df.

Figure 8: **Simulation:** Results of systematic search of open loop CPG-based control with imposed trot-like limb phases for $f = 0.25$ Hz.

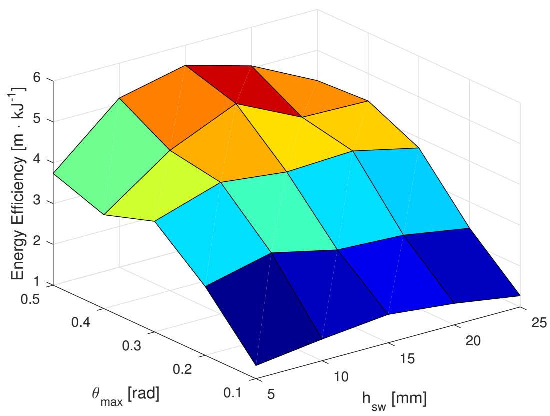

Figure 9: **Hardware:** Energy efficiency as a function of θ_{max} and h_{sw} – search performed for $f = 0.25$ Hz and $df = 0.5$.

for, or a value similar to the energetic cost of animal life should be kept, considering also the cost of being stopped, which depends on the current posture and corresponding motor torques. On the other hand, if the interest lies within the control of a specific robot, all the energetic consumption is ought to be accounted for, and in such a case, energetic cost in simulation should have an integrative base.

Given that energy efficiency is defined in equation 9 as total distance per energy unit, the integrative effect of base current will favor fast locomotion gaits, which in simulation, are much less energy efficient than slow ones.

Finally, despite the differences, similar primitives are possible to extract from simulation and hardware regarding trajectory. These are that a value of h_{sw} should be big enough to create a ground clearance (≈ 15 mm on hardware), but not higher, since this imposes an energetic cost without influence in speed.

5.3. Tegotae-based Control – Convergence to Trot

A first big challenge of this project was to achieve feasibility of convergence to trot gait from an arbitrary initial condition, with decentralized control of each limb by a Tegotae-based feedback rule. This was possible first on simulation, and later on hardware. In figure 10, 3-dimensional force measurements from *Optoforce* sensors, show such convergence with all limbs starting at the same phase. It is here observable the fast adaptation of the limb phases by physical communication, towards a stable periodic locomotion, as well as the appearance of an emergent duty factor.

Several initial conditions were tested on hardware, having always resulted in steady state trot gaits, which we have seen to be the most energy efficient. The speed of convergence from zero initial condition of all limbs was proven to decrease with σ, in the manner described in figure 11.

5.4. Tegotae-based Control – Steady State

In a first analysis, the results of experiment 4, performed in simulation, were collected, having encountered similar conclusions in terms of trajectory, inside a linear regime, but a lot of unstable or noisy results outside. A reduction of workspace exists, mainly due to noisy feedback, resulting on unstable time responses for high values of θ_{max}. This effect is emphasized for higher frequencies.

Very low values of σ seem to be the most energy efficient, as well as the fastest for a given trajectory. However, higher attraction allows a linear regime in an increased range of θ_{max}.

Focusing on the effect of this attraction coefficient σ, in the steady state time response of the system, an acceleration on phase emerges during $\phi_i \in [0, \pi/2]$, and a deceleration during $\phi_i \in [\pi/2, \pi]$. However, the overall attraction tends to slow down

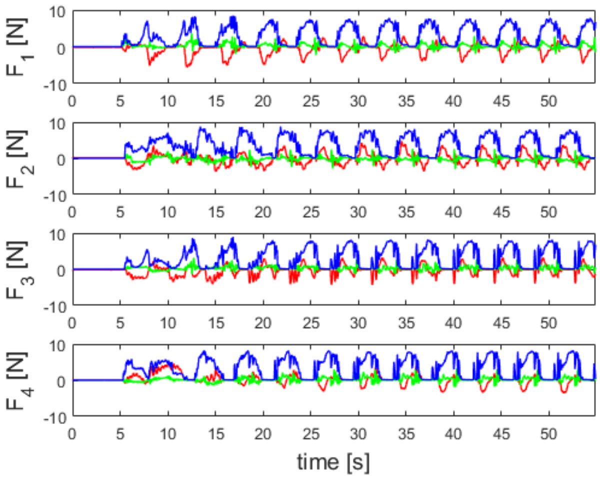

Figure 10: **Hardware:** Force measurements of each limb i (F_{ix} in red, F_{iy} in green and F_{iz} in blue) showing convergence to limit cycle behaviour correspondent to trot – All limbs in phase initially, and $\sigma = 0.1$.

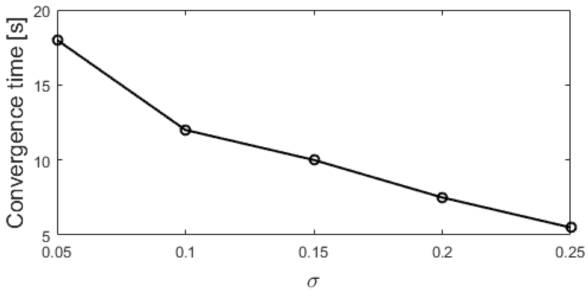

Figure 11: **Hardware:** Convergence time from limbs in-phase to steady state trot dependent of attraction coefficient σ.

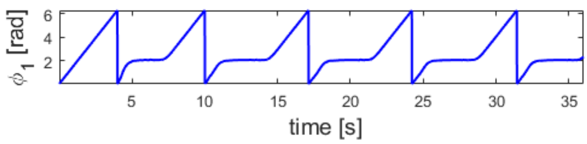

Figure 12: **Hardware:** Phase evolution with high attraction coefficient $\sigma = 0.5$ for $f = 0.25$ Hz.

the locomotion speed, and affect energy efficiency. An experiment performed on hardware that shows the effect of high attraction coefficient are exhibited in figure 12.

Considering now the way equation 2 imposes attraction trough the coefficient σ, it is intuitive that at higher frequencies f, an equal value of σ will have a decreased effect. As normal forces N_i prove to be independent of frequency (verified), scaling properties of σ with frequency should be observable.

To clearly visualize this effect, a systematic search with intervals of σ scaled with frequency was performed, resulting on figure 15.

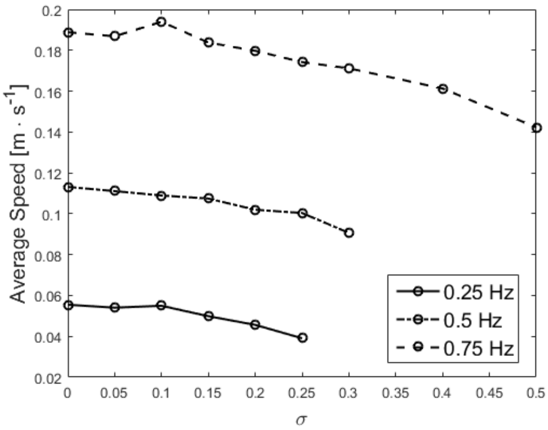

(a) Average speed – $\overline{v_{CM}}$.

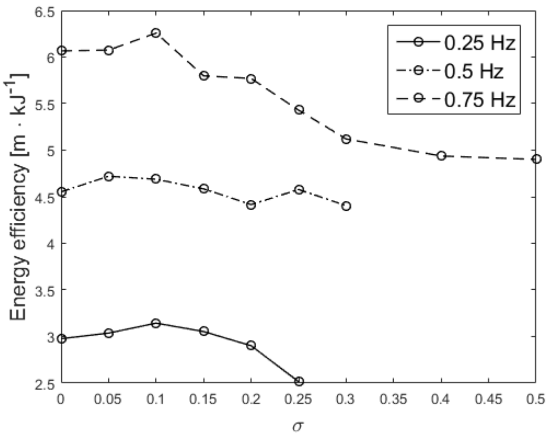

(b) Energy efficiency – ϵ_t.

Figure 13: **Hardware:** Analysis of effect of frequency and σ on average speed and energy efficiency – $\sigma = 0$ corresponds to imposed trot gait.

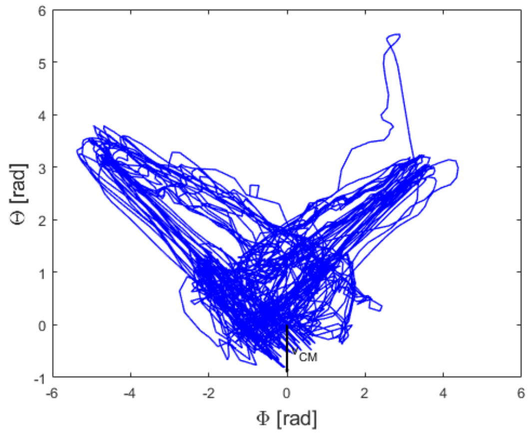

(a) Open loop trot gait: $\sigma = 0$.

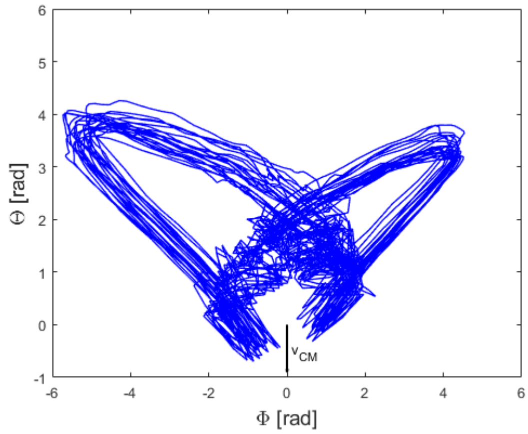

(b) Closed loop gait with $\sigma = 0.3$.

Figure 14: **Hardware:** Comparison between open and closed loop pendular behaviours observed in roll (Φ) *versus* pitch (Θ) – frequency $f = 0.75$ Hz.

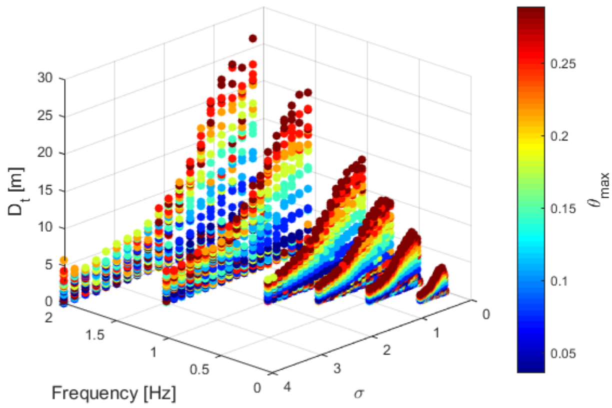

Figure 15: **Simulation:** Systematic search with σ range scaled with frequency – Clear indication that σ should be scaled with frequency.

With the goal of deriving reliable conclusions, the hardware experiments 7 were performed, including different values of σ, tested at 3 frequencies $f \in (0.25, 0.5, 0.75)$ Hz. The results of these experiments are exhibited in figure 13, where the negative effect of attraction on average speed can be seen, inducing a slight quasi-linear decay, with some traces of scaling.

In terms of energy efficiency, it is important to note that decentralized control of each limb by a Tegotae rule, was able not just to drive the system towards a stable gait, as it forced convergence to gaits even more efficient than imposed trot. This was acquired by the emergence of a duty factor closer to the optimum, and by real time adjustments to perturbations or non-symmetries on the system dynamics.

As previously introduced, there is a big difference between energy computation in simulation and hardware, which here plays an important role as well. The integrative base current favors faster gaits, explaining the higher energy efficiency curves of the top frequencies. Additionally, because of such phenomena, high values of σ are penalized in energy efficiency. Having this in mind, and looking at figure 13(b), there seems to be an increase of the near-optimum region.

Besides allowing the emergent convergence from any initial condition to solutions which are very close to optimal in terms of efficiency, the simple Tegotae feedback rule also increases robustness of the system to perturbations. This effect can be observed in the limit cycle behaviour of the experiments correspondent to $\sigma = 0$ and $\sigma = 0.3$ – figure 14. In open loop, the transition from swing to stance phase is not smooth, with collisions against the ground that affect mechanical stability and direction of locomotion. However, with the introduction of σ, the gait becomes much more stable, with smoother stepping and body motion – figure 14(b).

5.5. Binary Tegotae

As a final question to be answered in this project, the approach given by equation 3 was tested, having resulted in similar capabilities in terms of emergent locomotion. One drawback, found at low frequencies, is that the hard-filtering imposed by a force threshold, does not let the noise play a helpful role in diverging from an unstable limit cycle. This was found to be true for the case of in-phase initialization of all limbs, where an external perturbation is needed to repel the system from a locally stable limit cycle.

Despite the similar capabilities, when carefully analyzed, binary feedback induces undesired losses in performance. This can be seen in convergence time, where this strategy requires more than double of the times presented in figure 11 – table 2, and in steady state speed and efficiency – table 3.

It is therefore clear that some relevant information is lost by considering binary feedback, being however enough to generate physical communication and emergent locomotion.

Table 2: Convergence times for hardware experiments on binary feedback at different frequencies.

Frequency [Hz]	Convergence time [s]
0.25	43
0.5	41

Table 3: Binary *versus* normal feedback in terms of steady state speed and energy efficiency.

Feedback type	$\overline{v_{CM}}[m \cdot s^{-1}]$	$\epsilon_t[m \cdot kJ^{-1}]$
$\sigma = 0.1$	0.0559	3.146
$\sigma_b = 0.6$	0.0458	2.619

6. Conclusions

During the initial iterative processes performed to allow the achievement of convergence to steady state locomotion behaviours, some problems were identified regarding the control of modular structures, being the main problem is dynamical stability. The weight distribution of the robot and inertial characteristics play a very important role, and robust mechanics is essential to provide the necessary stability in transient phases.

Having the mentioned mechanical properties, and with use of a simple parametrization method proposed in this work, it is shown that a CPG-based control approach can result in many gaits found in nature, where walking gaits are more stable at low speeds and running gaits at high velocities. Walking trot is proven to be the most energy efficient way of locomotion for our robotic platform, and in comparison with [11] this shows that spinal compliance plays an important role in walking gaits such as D-S walk and L-S walk. The fact that no other gait besides trot was achieved by the decentralized approach, as done in [10], also reveals that compliance is crucial for dynamical running gaits.

Regarding step trajectory followed in open loop, it was possible to extract general principles for performance. Having a stretched knee during stance phase, and imposing a duty factor slightly above 0.5 increases energy efficiency. Having a swing phase characterized by the minimum ground clearance necessary to avoid stumbling is desired (≈15 mm for hip amplitudes up to 1 rad). The traveling speed is proportional to hip amplitude and frequency.

During the project development, a lot of differences were encountered between simulation and hardware, being the most relevant the different computation of energetic cost. A correct choice of a base cost for no movement is crucial and directly linked to the goal of the study. Knowing that stopped motors consume energy, and that standing in diverse postures has different associated consumption, a base cost should have a term purely dependent on the torque.

In the case of Tegotae, it was shown that a decentralized control of each limb, driven by sensory feedback, can result in convergence from any initial condition to a steady state limit cycle behaviour. Additionally, the resulting gait proves to be even more energy efficient than induced trot due to underlying effects that include emergent duty factor and increased robustness to perturbations.

High values of attraction coefficient σ are beneficial for fast convergence from an arbitrary initial condition to a dynamically stable limit cycle, however after transient, high attraction proves to reduce speed and energy efficiency, even if mechanical stability is increased. Hence, a non-constant value of

σ should be used for control purposes. If the optimal gait is known, an attraction proportional to to the difference between current and desired limb phases should be used, leading to a Tegotae rule similar to equation 10, where σ_c refers to constant sigma. In a general case, not knowing the optimal gait, an exponential decay of σ with time should be considered.

$$\dot{\phi_i} = \omega + \sigma_c \cdot \sum_j (\phi_j - \phi_i - \psi_{ij}) \cdot N_i \cos\phi_i \quad (10)$$

In addition, scaling properties of the attraction coefficient with frequency were observed, implying that this effect should also be accounted for in the design of a Tegotae rule, proposing equation 11.

$$\dot{\phi_i} = \omega \left(1 + \sigma_c \cdot \sum_j (\phi_j - \phi_i - \psi_{ij}) \cdot N_i \cos\phi_i\right) \quad (11)$$

Finally, binary feedback proved to be enough to drive the system towards steady state locomotion, having however loss of relevant information with consequences in convergence time, and steady state performance.

This thesis work represented an initial phase of a wider project, having included the implementation of software and hardware tools to be used in future studies and experiments.

Acknowledgements
The author would like to thank Paulo Oliveira, Auke Ijspeert, Simon Hauser and Florin Dzeladini for supervising this project with remarkable availability, the hole team at Biorobotics Laboratory of EPFL for multiple helps, and family and friends for unconditional support.

References

[1] Auke Jan Ijspeert, Alessandro Crespi, Dimitri Ryczko, and Jean-Marie Cabelguen. From Swimming to Walking with a Salamander Robot Driven by a Spinal Cord Model. *Science*, 315(5817):1416–1420, March 2007.

[2] Yasuhiro Fukuoka, Hiroshi Kimura, and Avis H. Cohen. Adaptive Dynamic Walking of a Quadruped Robot on Irregular Terrain Based on Biological Concepts. *The International Journal of Robotics Research*, 22(3-4):187–202, March 2003.

[3] C. Liu, Q. Chen, and D. Wang. CPG-Inspired Workspace Trajectory Generation and Adaptive Locomotion Control for Quadruped Robots. *IEEE Transactions on Systems, Man, and Cybernetics, Part B (Cybernetics)*, 41(3):867–880, June 2011.

[4] Jiaqi Zhang, Feng Gao, Xiaolei Han, Xianbao Chen, and Xueying Han. Trot Gait Design and CPG Method for a Quadruped Robot. *Journal of Bionic Engineering*, 11(1):18–25, January 2014.

[5] Jiang Shan, Cheng Junshi, and Chen Jiapin. Design of central pattern generator for humanoid robot walking based on multi-objective GA. In *2000 IEEE/RSJ International Conference on Intelligent Robots and Systems, 2000. (IROS 2000). Proceedings*, volume 3, pages 1930–1935 vol.3, 2000.

[6] Carla M. A. Pinto and Martin Golubitsky. Central pattern generators for bipedal locomotion. *Journal of Mathematical Biology*, 53(3):474–489, July 2006.

[7] Gen Endo, Jun Morimoto, Takamitsu Matsubara, Jun Nakanishi, and Gordon Cheng. Learning CPG-based Biped Locomotion with a Policy Gradient Method: Application to a Humanoid Robot. *The International Journal of Robotics Research*, 27(2):213–228, February 2008.

[8] J. Fang, Y. Ren, and D. Zhang. A robotic exoskeleton for lower limb rehabilitation controlled by central pattern generator. In *2014 IEEE International Conference on Robotics and Biomimetics (ROBIO)*, pages 814–818, December 2014.

[9] Auke Jan Ijspeert. Central pattern generators for locomotion control in animals and robots: A review. *Neural Networks*, 21(4):642–653, May 2008.

[10] Atsushi Tero, Masakazu Akiyama, Dai Owaki, Takeshi Kano, Akio Ishiguro, and Ryo Kobayashi. Interlimb neural connection is not required for gait transition in quadruped locomotion. *ResearchGate*, October 2013.

[11] Dai Owaki, Takeshi Kano, Ko Nagasawa, Atsushi Tero, and Akio Ishiguro. Simple robot suggests physical interlimb communication is essential for quadruped walking. *Journal of The Royal Society Interface*, 10(78):20120669, January 2013.

[12] Dai Owaki, Leona Morikawa, and Akio Ishiguro. Why do quadrupeds exhibit exclusively either trot or pace gaits? *Dynamic Walking Annual Meeting*, 2013.